ARL-MR-0887 • MAR-2015

US Army Research Laboratory

Stress Averaging for a Beam Network for Use in a Hierarchical Multiscale Framework

by Richard Becker and Adam Sokolow

NOTICES

Disclaimers

The findings in this report are not to be construed as an official Department of the Army position unless so designated by other authorized documents.

Citation of manufacturer's or trade names does not constitute an official endorsement or approval of the use thereof.

Destroy this report when it is no longer needed. Do not return it to the originator.

ARL-MR-0887 ● MAR 2015

US Army Research Laboratory

Stress Averaging for a Beam Network for Use in a Hierarchical Multiscale Framework

by Richard Becker and Adam Sokolow
Weapons and Materials Research Directorate, ARL

REPORT DOCUMENTATION PAGE

Form Approved
OMB No. 0704-0188

1. REPORT DATE *(DD-MM-YYYY)*	2. REPORT TYPE	3. DATES COVERED
March 2015	Final	1 September –31 December 2014

4. TITLE AND SUBTITLE
Stress Averaging for a Beam Network for Use in a Hierarchical Multiscale Framework

5a. CONTRACT NUMBER

5b. GRANT NUMBER

5c. PROGRAM ELEMENT NUMBER

6. AUTHOR(S)
Richard Becker and Adam Sokolow

5d. PROJECT NUMBER

5e. TASK NUMBER

5f. WORK UNIT NUMBER

7. PERFORMING ORGANIZATION NAME(S) AND ADDRESS(ES)
US Army Research Laboratory
ATTN: RDRL-WMP-C
Aberdeen Proving Ground, MD 21005-5069

8. PERFORMING ORGANIZATION REPORT NUMBER
ARL-MR-0887

9. SPONSORING/MONITORING AGENCY NAME(S) AND ADDRESS(ES)

10. SPONSOR/MONITOR'S ACRONYM(S)

11. SPONSOR/MONITOR'S REPORT NUMBER(S)

12. DISTRIBUTION/AVAILABILITY STATEMENT
Approved for public release; distribution is unlimited.

13. SUPPLEMENTARY NOTES

14. ABSTRACT
An efficient procedure for obtaining the average stress within a representative volume element (RVE) composed of beam elements is developed and validated. A model composed of a network of elastic beam elements is taken as the lower length scale in a hierarchical modeling framework for dynamic analyses. An efficient procedure for attaining the static equilibrium configuration of the RVE is presented. An algorithm for determining the average stress within the RVE based on the virtual work principle is assessed by comparison with either the total elastic energy within the RVE or the summation of surfaces forces over the RVE boundary. The results from the virtual work stress computation algorithm are in good agreement with the more direct calculations, including those with inelastic deformation, indicating that it is appropriate for analysis of a lower length scale model in a hierarchical modeling framework.

15. SUBJECT TERMS
multiscale, RVE, beam, unit cell, virtual work

16. SECURITY CLASSIFICATION OF:			17. LIMITATION OF ABSTRACT	18. NUMBER OF PAGES	19a. NAME OF RESPONSIBLE PERSON
a. REPORT	b. ABSTRACT	c. THIS PAGE	UU	28	Richard C Becker
Unclassified	Unclassified	Unclassified			19b. TELEPHONE NUMBER (Include area code) 410-278-7980

Standard Form 298 (Rev. 8/98)
Prescribed by ANSI Std. Z39.18

Contents

List of Figures

List of Tables

Acknowledgments

This work has been supported through the US Army Research Laboratory Enterprise for Multiscale Research in Materials.

INTENTIONALLY LEFT BLANK.

1. Introduction

Networks of finite element beam elements are being explored as a means of representing trabecular bone structure in an adaptive hierarchical multiscale (HMS) simulation framework. The beams are intended to comprise a representative volume element (RVE) at the lower length scale, which is interrogated to produce a response used by a discretized skeletal model at the higher length scale. Use of a beam network will facilitate representation of an anisotropic structure and variations in bone density by modifying the beam arrangement and cross-sectional properties. The hierarchical multiscale framework is described in detail by Knap et al.[1]

In the hierarchical multiscale framework, the models functioning at both the higher and lower length scale exchange information. For the coupled finite element models considered here, the lower length scale model replaces the constitutive evaluation in the higher length scale code. Consistent with this treatment as a constitutive model, the higher length scale model provides a set of history variables and the velocity gradient to drive the lower length scale model, and the lower length scale model returns Cauchy stress and updated values of the history variables. A consistent scheme is needed for specifying boundary conditions on the RVE and determination of the average Cauchy stress from the lower length scale model. These 2 tasks are the focus of this report.

In the construct of the hierarchical multiscale framework, the lower length scale model does not persist from one time step to the next. Their persistence would require that all lower length scale models run throughout the entire simulation and would be inconsistent with the efficiency objectives of the hierarchical multiscale framework.[1] Instead, for each time step, the lower length scale model is reinstantiated to a deformed state that is consistent with the end of the previous time step. The reinstantiation must be accomplished using a reduced set of information carried by the higher length scale model. The reduction and reinstantiation procedure is a research area itself for the many applications of the hierarchical multiscale framework, as the solution is often path-dependent. However, for a narrower set of simulations in which the material and geometric responses are independent of deformation path, only the end state needs to be specified. The small-strain, linear elastic examples used in the following demonstration problems are assumed to be path-independent.

The selection of an appropriate RVE is also a research topic that will not be addressed here. The term “representative volume element” is used in the most general sense of representing a volume of material. There is no implication that the

homogenized response of the model has converged with respect to increasing the volume of material represented. For irregular structures, and particularly for those with gradients, such convergence may never be reached. There are also potential issues that arise from an insufficient number of beams within the RVE and networks of beams whose connectivity results in otherwise degenerate structures. Such instances reflect resolution issues and model construction, and those types of sparse or degenerate beam networks are not considered at this time.

The purpose of this memorandum is to document and validate the choices made for applying boundary conditions to, and extracting Cauchy stress from, a network of elastic beams comprising an RVE for use within the hierarchical multiscale framework.[1] While it has been shown that a consistent reduction of a regular network of beams can lead to higher order gradient models,[2] the determinations herein are restricted to simple volume averages that are consistent with traditional finite element codes that may be used as the higher length scale model. Higher order representations are not considered. The stress averaging outlined in the following was not found in a cursory search of the literature, but such virtual work approaches are standard practice and there is no assumption that it is original or unique.

Vectors and second-rank tensors are represented by bold face Latin and Greek characters, respectively. A raised dot operator indicates an inner product, and a colon operator signifies a trace of the inner product of 2 second-rank tensors, a contraction. All summations are explicitly indicated, and no summation convention is assumed.

Unit vectors along the beam directions are expressed in terms of the coordinate direction base vectors as follows:

$$\boldsymbol{r} = r_x\boldsymbol{e}_x + r_y\boldsymbol{e}_y + r_z\boldsymbol{e}_z. \tag{1}$$

$$\boldsymbol{s} = s_x\boldsymbol{e}_x + s_y\boldsymbol{e}_y + s_z\boldsymbol{e}_z. \tag{2}$$

$$\boldsymbol{t} = t_x\boldsymbol{e}_x + t_y\boldsymbol{e}_y + t_z\boldsymbol{e}_z. \tag{3}$$

The direction of the beam axis is denoted by the unit vector $\boldsymbol{r}$, and $\boldsymbol{s}$ and $\boldsymbol{t}$ denote an orthogonal pair of vectors that are also orthogonal to the beam axis. $\boldsymbol{e}_x$, $\boldsymbol{e}_y$, and $\boldsymbol{e}_z$ are the unit vectors along the global Cartesian coordinate axes, and scalar projections such as $r_x = \boldsymbol{r} \cdot \boldsymbol{e}_x$ are direction cosines of the beam unit vectors.

2. Lower Length Scale Model

A multitude of finite element codes and beam elements can be used for the beam model, and the boundary conditions and stress averaging methods described here should be straightforward to apply to many of them. The Lawrence Livermore

National Laboratory's ParaDyn code is used within the HMS framework, so it is an obvious choice for the present evaluations. ParaDyn is available on US Department of Defense (DOD) high-performance computing machines without restrictions on the number of simultaneous executions. It has fast initialization and execution, robust algorithms, and xdmf/hdf5 data files for ease of extracting requisite information.

ParaDyn is an explicit dynamic code where the dynamic stress equilibrium equations are solved by a second order accurate time integration algorithm, and information is propagated through the structure by stress waves. The time step is limited by the Courant-Friedrichs-Lewy condition to approximate the time it takes a wave to traverse an element. Hence, many small time steps are required for the solution to approach a quasi-static equilibrium configuration as waves reverberate within the model domain. The waves and dynamic modes persist unless quieted by some form of damping. The initialization method and damping described in the following will minimize these dynamic effects and reduce the number of time steps required to obtain a quiescent solution.

Beam networks are generated from nodes that exist either on the exterior boundary of the RVE or in the interior of the RVE. These exterior and interior nodes, and their connectivity, form the beam networks of the lower length scale model. Unlike continuum RVE models where the entire exterior of the RVE is populated by nodes, beam structures do not necessarily define a nice box with nodes on edges and corners. Beams will intersect the RVE surface at multiple angles and could slide considerably along the surface if constrained only in the direction of the surface normal. This would create a locally high average deformation on the surface inconsistent with the applied boundary conditions. Hence, all degrees of freedom of all exterior nodes are constrained.

The specific beam element used in the evaluations is the Hughes-Liu beam, which is derived from a consistent reduction of a shell element.[3] The beam supports axial forces, shear forces, bending moments, and torsion. The beams can have an arbitrary cross-section shape (integrated with Gaussian quadrature) and can also have a linear taper along their length. Only circular beams of constant cross section are used in this study. The method presented will be applicable to arbitrary beam cross sections, but additional work will be needed to determine the accuracy of the method for tapered beams.

Certain assumptions about the stress distribution are built into the beam elements. While stress components given with respect to the beam axes represent the stress in the beam, it is not a detailed stress field. For example, the parabolic shear stress distribution across the beam section is represented by an average, and there is no

counterpart to this shear stress resolved along the beam axis. Consequently, standard continuum tensor transformations and stress averaging do not apply because of assumptions associated with the dimensional reduction. This is discussed further in Section 4.

3. Reinstatiating the Beam Network

Within the HMS framework, a reduced set of information is supplied to the lower length scale model. This information is used to first reinstantiate the model to its prior state and then deform it to the current state. However, this process can result in unstable numerical behaviors if the path-dependence is important and not taken into account. For the problems considered here, linear elastic networks of beams are subjected to small deformations. Elastic solutions are path-independent provided the path taken does not encounter a material or geometrically driven bifurcation point, such as buckling. With the small deformations and the relatively small beam networks considered in the following simulations, no bifurcation points are expected in the vicinity of the deformed configuration, so the final state is assumed to be independent of deformation path. This assumption simplifies the reinstatiation problem to working only with the initial beam configuration and the current deformation specified by the higher length scale model.

To ensure that the deformation applied to the model is consistent with the deformation of the higher length scale model in an HMS scheme, all of the nodes on the exterior of the beam network model are moved to points determined by their initial coordinates and the applied deformation gradient. However, abruptly moving the exterior nodes to the proper locations would create dynamic effects on the interior of the model when using the explicit time integration scheme. Alternatively, moving the exterior nodes slowly enough to avoid these inertial effects would be unacceptably time consuming. The approach presented here is to move both the exterior and the interior nodes to positions consistent with the applied deformation and then to remove the constraint from these interior nodes. This allows the coordinates to be initialized to the average deformed configuration using just a few time steps, and the subsequent dynamic solution is essentially an energy minimization from that uniform strain state with the exterior nodes fixed.

Since the beams are elastic, the dynamic motion of the interior will persist unless some form of dissipation is applied. Here, a viscous force is applied to the nodes through a mass proportional damping algorithm available in ParaDyn. This is a nonconservative force, but because the desired quasi-static solution is path-independent, the precise deformation history and energy loss do not affect the solution. There are 2 parameters required for the mass proportional damping option:

the peak damping frequency and the fraction of critical damping. The frequency can be estimated by observing an undamped simulation and the fraction of critical damping is chosen to be 0.9 to allow modest overshoot while settling into the static equilibrium configuration.

4. Cauchy Stress Determination from Virtual Work

Several approaches can be used to determine the average stress over the RVE beam model. The most obvious may be summing forces over boundaries, but there are potential issues because the deformation is applied to all of the exterior nodes. The exterior forces in the 3 coordinate directions will sum to zero, but normal forces on opposite faces of the RVE may sum to different values because of tangential forces on the remaining surfaces. This does not produce a well-defined average stress. Similarly, tangential forces on corresponding faces may not balance to produce a symmetric shear stress.

Here a volume averaging method based on virtual work will be employed. It is motivated by volume averaging stress components in continuum models,[4] but the implementation details are somewhat different when applied over beam structures. The method assumes that an equilibrium solution has been established for the beam network in the RVE. The average stress of the RVE, $\overline{\boldsymbol{\sigma}}$, is then constructed to have the same virtual work, $\delta\phi$, as the beam network when subjected to a common, work-conjugate virtual strain, $\delta\boldsymbol{\varepsilon}$**.** The virtual work is the integral of mechanical work over the RVE. More specifically, it is the volume integral of the contraction of the Cauchy stress tensor with the work conjugate virtual strain tensor. For a constant average stress over the RVE, the volume integral can be reduced to a simple multiplication by the RVE volume.

$$\delta\phi = \int_V \boldsymbol{\sigma}\colon \delta\boldsymbol{\varepsilon}\, \mathrm{d}v \;\equiv\; \overline{\boldsymbol{\sigma}}\colon \delta\boldsymbol{\varepsilon}\, V. \tag{4}$$

Since each beam is a discrete element, the virtual work on the network is determined by summing the contributions from the individual virtual work from each beam element.

$$\delta\phi = \sum_1^{N-Beams} \int_{v_{Beam}} \boldsymbol{\sigma}^{Beam}\colon \delta\boldsymbol{\varepsilon}\, \mathrm{d}v. \tag{5}$$

Consistent with the development of beam models, the virtual work is projected into an orthogonal coordinate system aligned with the beam, and the volume integration is decomposed into integrals over the beam cross-sectional area, a, and the beam length, l.

$$\delta\phi = \sum_1^{N-Beams} \int_{l_{Beam}} \int_{a_{Beam}} (\sigma_A \delta\varepsilon_A + \tau_S \delta\gamma_S + \tau_T \delta\gamma_T)\, \mathrm{d}a\, \mathrm{d}l, \qquad (6)$$

where σ_A is the stress distribution along the beam axis and τ_S and τ_T are shear stress distributions over the beam cross section along the local orthogonal directions *S* and *T*, respectively. The virtual strain has likewise been projected in this local beam coordinate system with $\delta\varepsilon_A$ being the projection along the beam axis and $\delta\gamma_S$ and $\delta\gamma_T$ being shear strains in the *S* and *T* directions. The shear strains correspond to gradients along the beam axis of virtual displacements in the *S* and *T* directions. Shear displacements along the beam axis are not captured by beam elements.

The beam cross-sectional area is assumed to be constant over the length of the beam, which allows the beam length to be integrated separately. The integration of the stress over the cross section is accomplished by numerical quadrature for the Hughes-Liu beam element in ParaDyn. The cross-section integration produces forces in the beam coordinate direction such that the virtual work is reduced to a summation over all of the beams in the RVE.

$$\delta\phi = \sum_1^{N-Beams} l\, (F_A \delta\varepsilon + F_S \delta\gamma_S + F_T \delta\gamma_T). \qquad (7)$$

The integrated forces F_A, F_S, and F_T appearing in Eq. 7 are available in the ParaDyn output.

The virtual work of the unknown average stress, $\bar{\boldsymbol{\sigma}}$, represented by Eq. 4 is set equal to the virtual work given by the explicit summation over the beams in Eq. 7. Then, by virtue of the virtual strains being arbitrary, the average stress can be determined. Determining the components of the average stress requires that the projections of the virtual strain tensor appearing in Eq. 7 be expressed as components along the global Cartesian coordinate axes.

The virtual strain along the beam axis can be obtained by a straightforward projection of the strain tensor. The definitions of the projected shear strains must be consistent with the virtual work expression for beam elements, Eq. 7. The displacements accompanying the virtual shear strains are orthogonal to the beam axes with no displacements along the beam axes. This is reminiscent of simple shear by $\delta\gamma$. Thus, when the virtual strain is projected to the beam coordinates, only the component of the strain associated with displacement orthogonal to the beam axis contributes to the virtual work. These are

$$\delta\gamma_S = \boldsymbol{s} \cdot \delta\boldsymbol{\varepsilon} \cdot \boldsymbol{r} \text{ and } \delta\gamma_T = \boldsymbol{t} \cdot \delta\boldsymbol{\varepsilon} \cdot \boldsymbol{r}. \qquad (8)$$

The virtual strains projected along the beam axis, $\boldsymbol{r}$, and in the $\boldsymbol{s}$ and $\boldsymbol{t}$ directions are expressed as components along the global Cartesian coordinate axes using the definitions of the beam vectors from the notation section.

$$\begin{aligned}\delta\varepsilon_A = \boldsymbol{r}\cdot\delta\boldsymbol{\varepsilon}\cdot\boldsymbol{r} = {} & r_x\boldsymbol{e}_x\cdot\delta\boldsymbol{\varepsilon}\cdot\boldsymbol{e}_x r_x + r_y\boldsymbol{e}_y\cdot\delta\boldsymbol{\varepsilon}\cdot\boldsymbol{e}_y r_y + r_z\boldsymbol{e}_z\cdot\delta\boldsymbol{\varepsilon}\cdot\boldsymbol{e}_z r_z \\ & +2\,r_y\boldsymbol{e}_y\cdot\delta\boldsymbol{\varepsilon}\cdot\boldsymbol{e}_z r_z + 2\,r_z\boldsymbol{e}_z\cdot\delta\boldsymbol{\varepsilon}\cdot\boldsymbol{e}_x r_x + 2\,r_x\boldsymbol{e}_x\cdot\delta\boldsymbol{\varepsilon}\cdot\boldsymbol{e}_y r_y \\ = {} & r_x^2\delta\varepsilon_{xx} + r_y^2\delta\varepsilon_{yy} + r_z^2\delta\varepsilon_{zz} + 2\,r_y r_z\delta\varepsilon_{yz} + 2\,r_z r_x\delta\varepsilon_{zx} + 2\,r_x r_y\delta\varepsilon_{xy}.\end{aligned} \tag{9}$$

$$\begin{aligned}\delta\gamma_S = \boldsymbol{s}\cdot\delta\boldsymbol{\varepsilon}\cdot\boldsymbol{r} \;\; & r_x s_x\delta\varepsilon_{xx} + r_y s_y\delta\varepsilon_{yy} + r_z s_z\delta\varepsilon_{zz} + \left(r_y s_z + s_y r_z\right)\delta\varepsilon_{yz} \\ & +(r_z s_x + s_z r_x)\delta\varepsilon_{zx} + \left(r_x s_y + s_x r_y\right)\delta\varepsilon_{xy.}\end{aligned} \tag{10}$$

$$\begin{aligned}\delta\gamma_T = \boldsymbol{t}\cdot\delta\boldsymbol{\varepsilon}\cdot\boldsymbol{r} = {} & r_x t_x\delta\varepsilon_{xx} + r_y t_y\delta\varepsilon_{yy} + r_z t_z\delta\varepsilon_{zz} + \left(r_y t_z + t_y r_z\right)\delta\varepsilon_{yz} \\ & +(r_z t_x + t_z r_x)\delta\varepsilon_{zx} + \left(r_x t_y + t_x r_y\right)\delta\varepsilon_{xy.}\end{aligned} \tag{11}$$

Substituting Eqs. 9–11 into Eq. 7, the virtual work expression for the beam network is

$$\begin{aligned}\delta\phi = \sum_{1}^{N-Beams} {} & \left[\left(F_A r_x^2 + F_s r_x s_x + F_t r_x t_x\right) l\;\delta\varepsilon_{xx}\right. \\ & + \left(F_A r_y^2 + F_s r_y s_y + F_t r_y t_y\right) l\;\delta\varepsilon_{yy} \\ & + \left(F_A r_z^2 + F_s r_z s_z + F_t r_z t_z\right) l\;\delta\varepsilon_{zz} \\ & + \left(2\,F_A r_y r_z + F_s r_y s_z + F_s r_z s_y + F_t r_y t_z + F_t r_z t_y\right) l\;\delta\varepsilon_{yz} \\ & + \left(2F_A r_z r_x + F_s r_x s_z + F_s r_z s_x + F_t r_x t_z + F_t r_z t_x\right) l\;\delta\varepsilon_{zx} \\ & \left. + \left(2F_A r_x r_y + F_s r_x s_y + F_s r_y s_x + F_t r_x t_y + F_t r_y t_x\right) l\;\delta\varepsilon_{xy}.\right.\end{aligned} \tag{12}$$

Eq. 12 is simplified by introducing:

$$\begin{aligned}F_x &= F_A\,r_x + F_s\,s_x + F_t\,t_x \\ F_y &= F_A\,r_y + F_s\,s_y + F_t\,t_y \\ F_z &= F_A\,r_z + F_s\,s_z + F_t\,t_z\,,\end{aligned} \tag{13}$$

so that the expression for virtual work, Eq. 7, becomes

$$\begin{aligned}\delta\phi = \sum_{1}^{N-Beams} {} & l\left[F_x r_x\delta\varepsilon_{xx} + F_y r_y\delta\varepsilon_{yy} + F_z r_z\delta\varepsilon_{zz}\right. \\ & \left.+\left(F_y r_z + F_z r_y\right)\delta\varepsilon_{yz} + (F_z r_x + F_x r_z)\delta\varepsilon_{zx} + \left(F_x r_y + F_y r_x\right)\delta\varepsilon_{xy}\right].\end{aligned} \tag{14}$$

Recalling the right-hand side of Eq. 4, the virtual work of the average stress over the RVE subjected to the same virtual strain is expanded explicitly as

$$\begin{aligned}\delta\phi &= \bar{\boldsymbol{\sigma}}:\delta\boldsymbol{\varepsilon}\,V \\ &= \left[\bar{\sigma}_{xx}\delta\varepsilon_{xx} + \bar{\sigma}_{yy}\delta\varepsilon_{yy} + \bar{\sigma}_{zz}\delta\varepsilon_{zz} + 2\,\bar{\sigma}_{yz}\delta\varepsilon_{yz} + 2\,\bar{\sigma}_{zx}\delta\varepsilon_{zx} + 2\,\bar{\sigma}_{xy}\delta\varepsilon_{xy}\right]V.\end{aligned} \tag{15}$$

Since Eqs. 14 and 15 are equal and the virtual strains are arbitrary, any one of the strain components can be nonzero while setting the rest to zero. The stress components for the RVE can then be determined by simply matching terms between Eqs. 14 and 15. Thus the average Cauchy stress components determined from the virtual work approach are

$$
\begin{aligned}
\bar{\sigma}_{xx} &= \frac{1}{V} \sum_{1}^{N-Beams} F_x \, r_x \, l \; ; \\
\bar{\sigma}_{yy} &= \frac{1}{V} \sum_{1}^{N-Beams} F_y \, r_y \, l \; ; \\
\bar{\sigma}_{zz} &= \frac{1}{V} \sum_{1}^{N-Beams} F_z \, r_z \, l \; ; \\
\bar{\sigma}_{yz} &= \frac{1}{V} \sum_{1}^{N-Beams} 0.5 \, (F_y r_z + F_z \, r_y \, l \; ; \\
\bar{\sigma}_{zx} &= \frac{1}{V} \sum_{1}^{N-Beams} 0.5 \, (F_z r_x + F_x r_z) \, l \; ; \\
\bar{\sigma}_{xy} &= \frac{1}{V} \sum_{1}^{N-Beams} 0.5 \, \left(F_x r_y + F_y r_x\right) l \, .
\end{aligned}
\tag{16}
$$

These expressions only involve the forces within the beams, their deformed lengths and orientations, and the volume of the RVE. No constitutive assumptions were required for this derivation implying that the average stress calculation is applicable for any constitutive model. The reinstantiation procedure for these cases, however, would have to be revisited.

5. Verification Analyses

This section assesses the algorithm for determining the average stress within the RVE based on the virtual work principle (Eq. 16). Since the averaging process itself is the topic of this research, the best available comparisons to verify that it produces favorable results are comparison with either the total elastic energy within the RVE or the summation of surfaces forces over the RVE boundary. Analytical expressions are derived for simple cases; however, approximations are made for the more complicated examples. It is important to note that inaccuracies in comparisons between the average stress calculations and the validation approximations do not necessarily reflect poorly on the average stress calculation.

Rather, as will be demonstrated, the inaccuracies reveal limitations of the approximations used for the more complex geometries and therefore a limitation in the use of the approximations as a validation tool.

5.1 Beam Properties and Loading History

The beam properties and sizes used in the analysis were chosen for convenience and are not necessarily representative of trabecular bone properties. The diameter of the round cross section beams is 0.1 mm, and the Young's modulus is E = 400 MPa (MPa = N/mm^2). The yield stress is set to 100 MPa so that the structure remains elastic. Since the beam deformation is integrated through time, the logarithmic strain is consistent with the beam deformation.

In all cases, the peak velocity is applied to the RVE for 1 ms and is ramped to zero over the next 1 ms. This gives a total displacement in millimeters of 1.5 times the velocity in millimeters per microsecond. At 2 ms, the boundary conditions on the interior nodes are removed and the interior nodes are permitted to relax to their static equilibrium positions over the next 2 ms. In the following examples, the peak velocities are all less than 10^{-13} mm/ms at the end of the 4-ms total run time. This indicates that the mass proportional damping is functioning as intended to eliminate the dynamic modes. The nodes on the exterior remain at the locations prescribed earlier in the simulation.

5.2 Analytic and Linearized Energy Relations

Models of increasing complexity are analyzed to assess the validity of the average stress calculation. For the simplest configurations, the stress calculation is compared with the force summation. For the more complex beam configurations, the total elastic energy of the beams computed by ParaDyn is compared with the elastic energy integrated over the RVE.

$$e = \int_0^{\bar{\varepsilon}} [V(\boldsymbol{\varepsilon})\boldsymbol{\sigma}(\boldsymbol{\varepsilon}) : d\boldsymbol{\varepsilon}]. \tag{17}$$

The volume, V, and the stress, $\boldsymbol{\sigma}$, are both a function of strain. The integration limit, $\bar{\varepsilon}$, is the average RVE strain.

For deformations with one nonzero strain component, only a single conjugate stress component contributes to the energy. Thus, if the applied strain and energy are known, the energy can be used to validate the stress calculation. However, the stress is not necessarily linear in strain even though the beams themselves are linear elastic and the strains are not large. The geometry changes associated with the beam

motion introduce nonlinearities. Hence, the total beam energy can only be used as an approximate verification metric for the virtual stress calculation unless the nonlinearties of the system can be properly characterized.

If the detailed information on nonlinearities is unavailable or too costly to process, a linear dependence of stress on applied strain is typically a reasonable assumption for the energy in a linear elastic material. For uniaxial strain compression where ε_{ev} is the applied strain and σ_{ev} is the conjugate stress computed by Eq. 16, the energy is calculated by

$$e = \int_0^{\varepsilon_{ev}} \left[\sigma_{ev} \frac{\varepsilon}{\varepsilon_{ev}} A L_0 e^{\varepsilon} d\varepsilon \right]. \tag{18}$$

The exponential times the reference length accounts for the changing volume of the RVE.

5.3 Two-Beam Model

A simple 2-dimensional (2-D) model composed of 2 beams initially oriented at 45° with respect to the horizontal is constructed, with the deformed configuration shown in Fig. 1. The RVE represented by the bounding box is *H* (1 mm) in the *y*-direction and *W = 2H* (2 mm) in the *x*-direction. Uniaxial strain velocity boundary conditions are applied to force compression in the *y*-direction. The bottom nodes are fixed and the 2 upper nodes are constrained in the *x*-direction. The downward velocity at the upper surface is 0.01 mm/ms during the first millisecond so that the total vertical displacement at the upper nodes after the ramp down in velocity is 0.015 mm, consistent with the loading description in Sections 3 and 5.1.

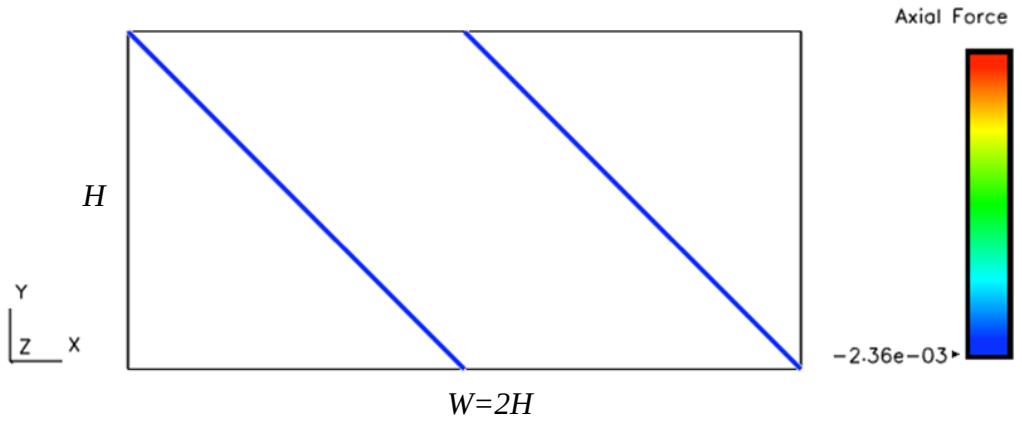

Fig. 1 Configuration for simple 2-beam model showing the axial force. *H* is the initial height (1 mm) and *W = 2H* is the initial width (2 mm).

5.3.1 Analytic Solution

The deformed beam length is

$$l = \left[(H-u)^2 + \left(\frac{W}{2}\right)^2\right]^{\frac{1}{2}} = H\,[(1-\tilde{u})^2+1]^{\frac{1}{2}}, \tag{19}$$

where u is the magnitude of the downward y-displacement, $\tilde{u}$ is the displacement normalized by the initial height, and $W = 2H$ has been utilized. To third order in $\tilde{u}$, the log strain in the beams is

$$\varepsilon = -\tfrac{1}{2}\left(\tilde{u} - \tfrac{1}{6}\tilde{u}^3\right). \tag{20}$$

The force in the vertical direction is related to the axial stress in the beams ($\sigma_A = E\,\varepsilon$), the beam area ($A$), and the current angle of the beam with respect to the horizontal (θ).

$$F_y = \sigma_A A\,\sin(\theta) = E\,\varepsilon\,A\,\frac{1-\tilde{u}}{[(1-\tilde{u})^2+1]^{\frac{1}{2}}} = -E\,A\,\frac{1}{2\sqrt{2}}\left(\tilde{u} - \frac{1}{2}\tilde{u}^2 - \frac{13}{24}\tilde{u}^3 + \cdots\right). \tag{21}$$

With an initial height (H) of 1 mm, the displacement (u) of 0.015 mm, and the given modulus and beam diameter, Eq. 21 gives a force of 0.016533824 N. The axial beam force computed by ParaDyn is shown in Fig. 1. Multiplying this by the sine of the current beam angle gives the same force as Eq. 21 to within 6 nonzero digits. There is deviation in the 7th, which is consistent with discarding terms $O(\tilde{u}^4)$ in the Eq. 21.

The average y-direction stress on the RVE is the force in y-direction, multiplied by 2 for the 2 beams and divided by 2 mm for the x-dimension of the RVE. A unit depth of 1 mm is assumed, so the y-direction stress consistent with Eq. 21 is –0.016533824 MPa. Analysis of the beams using Eq. 16 gives the same result, with deviation beginning in the 7th nonzero digit. Similarly, the x-direction stress (determined from the beam force, angle, and current RVE height) is –0.017041248 MPa and the shear stress is 0.016785629 MPa. Both agree with the results of Eq. 16 to the first 6 digits. Hence, the stress computation using the virtual work analysis of Eq. 16 is accurate for this simple case.

The energy per unit depth for the 2-D model is obtained for each beam by integrating the force times the differential displacement. The result is

$$e = E\,A\,\frac{1}{2\sqrt{2}}\left(\frac{1}{2}\,\tilde{u}^2 - \frac{1}{6}\tilde{u}^3 - \frac{13}{96}\tilde{u}^4 + \cdots\right). \tag{22}$$

The energy computed for 2 beams from the analytic energy relation, Eq. 22, for a displacement of 0.015 mm is $2.486474\text{x}10^{-4}$ N-mm, which is the same as the energy

integrated by ParaDyn to the 7 nonzero digits given. This establishes that a postanalysis integration of the energy can give the correct result if all of the nonlinearities are considered.

5.3.2 Approximate Energy Calculation

However, in an RVE constructed from a complex beam geometry, there will not be a closed-form solution, and it is important to know the magnitude of the error introduced by not directly accounting for nonlinearities. This will establish how such an energy metric could be expected to be in error when verifying whether the virtual work stress evaluated from Eq. 16 is a valid means of computing stress for more complex geometries.

For the previous example where $\varepsilon_{ev} = \ln(1 - 0.015)$, the linear energy approximation of Eq. 18 gives $e = 0.0074811\ A\ L_0\sigma_{ev}$ = 2.47383×10^{-4} N-mm, an error of 0.5%. A simpler approximation of $e = 0.5\ A\ L_0\sigma_{ev}\ \varepsilon_{ev}$ = 2.49887×10^{-4} N-mm also gives an error of 0.5%.

To demonstrate that this error is a result of the nonlinearities in the problem, the analysis is repeated with a displacement of 0.0015 mm, an order of magnitude smaller. Here the *y*-direction stress computed by the virtual work method, Eq. 16, is –0.00166483 MPa and the energy integrated numerically by ParaDyn is 2.49787x10^{-6} N-mm. Analytic Eqs. 21 and 22 reproduce these results to at least 6 nonzero digits. However, compared with the results of the 0.015-mm displacement, it is clear that the stress does not scale linearly with displacement, and the energy does not scale quadratically. The energy computed by the linear stress approximation of Eq. 18 is 2.49661x10^{-6} N-mm, an error of 0.025%, which is an order of magnitude smaller than with the larger displacement. These results are summarized in Table 1.

Table 1 Average RVE stress in the *y*-direction and total energy computed by various means for the configuration shown in Fig. 1. Digits that differ between stress predictions are highlighted. Digits of the energy predictions that differ from the ParaDyn solution are highlighted in yellow.

Displacement (mm)	Virtual work Eq. 16 (σ_{yy}, MPa)	Analytic Eq. 21 (σ_{yy}, MPa)	Analytic Eq. 22 (e, N-mm)	Linearized Eq. 20 (e, N-mm)	ParaDyn (e, N-mm)
0.0015	–0.00166483	–0.00166483	2.497871×10^{-6}	2.49661×10^{-6}	2.497872×10^{-6}
0.015	–0.0165338**5**	–0.0165338**2**	2.486474×10^{-4}	2.47383×10^{-4}	2.486474×10^{-4}

Hence, at the 0.015 strain level, errors of 0.5% in calculating the total energy using the linearized approximation of Eq. 18 are attributable to ignoring nonlinearities. If the computed energy is used as a validation metric for the virtual work stress calculations, agreement to within 0.5% in the total energy is the best that can be demanded.

5.4 Irregular Beam Structure in Compression

A 2-D model composed of 111 beams and 78 nodes, Fig. 2, is used for further validation of the virtual work stress calculation. The model extent is 2 × 2 mm in the plane, and a unit length out of plane is assumed. Boundary conditions consistent with uniaxial compression strain are applied as described in Section 5.1, with the total displacement on the upper surface being 0.015 mm. The axial stress distribution after the system has come to equilibrium is shown in Fig. 2.

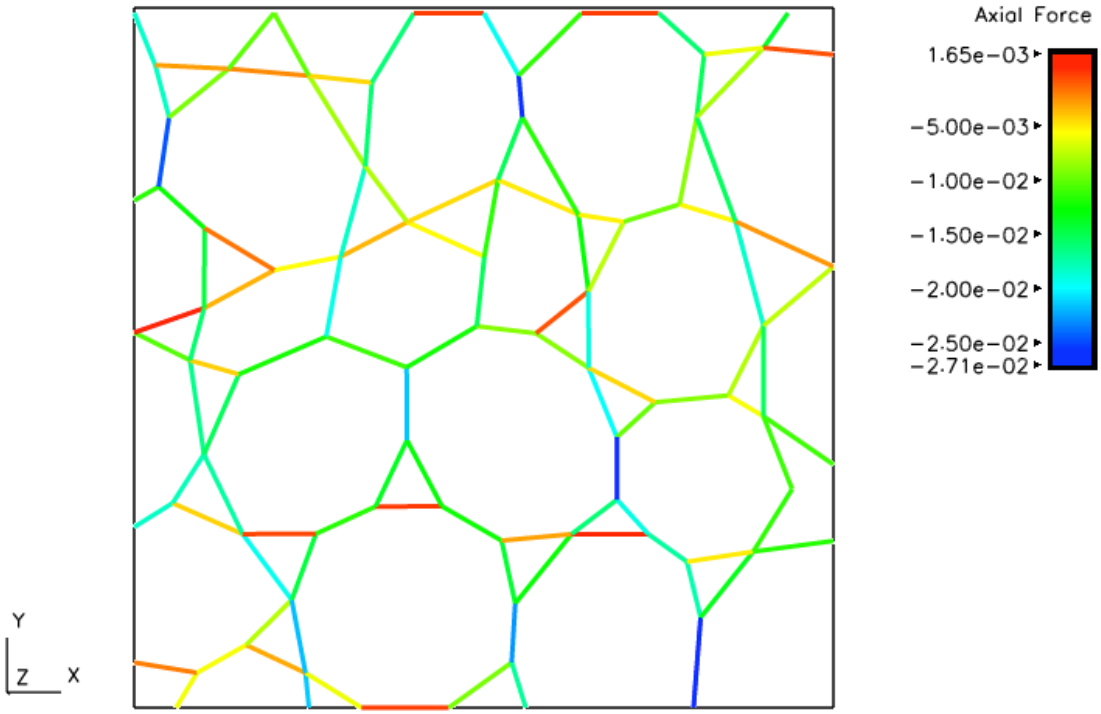

Fig. 2 Irregular beam configuration used to assess the stress calculation. The axial force is depicted. The region is 2 mm in both the *x* and *y* directions.

The *y*-direction stress from the virtual work relation, Eq. 16, is –0.04450714 MPa, and the full stress tensor is given in Table 2. Substituting this stress into the linearized energy relation, Eq. 18, with A = 2 mm^2, L_0 = 2 mm and $\varepsilon_{ev} = ln(1 - 0.015/2)$, the elastic deformation energy is estimated as 6.66769×10^{-4} N-mm. The integrated elastic energy computed by ParaDyn is 6.66622×10^{-4} N-mm, an energy

error of 0.02%. Therefore, the average stress for a complex RVE structure calculated by the virtual work expressions, Eq. 16, is consistent with the deformation energy.

Table 2 Computed stress for irregular beam structure

Stress Components for *y*-direction Strain (MPa)			Stress Components for Simple Shear (MPa)		
–0.01675563	0.00020244	0.0	0.00066804	0.01038036	0.0
0.00020244	–0.04450714	0.0	0.01038036	–0.00004881	0.0
0.0	0.0	0.0	0.0	0.0	0.0

Although the RVE is deformed in uniaxial strain, the *x*-direction stress and the *xy*-shear stress are nonzero. The *x*-direction stress corresponds to the stress resisting Poisson expansion. The shear stress results from the reaction of the structure to the applied deformation. The structure has normal-shear coupling, a natural tendency to shear under compression loading. However, since it is restrained by the applied boundary conditions, a reaction stress is produced. Neither of these stresses contributes to the macroscopic energy calculation since the associated strains are zero.

5.5 Irregular Beam Structure in Simple Shear

The same 2-D beam model shown in Fig. 2 is subjected to simple shear boundary conditions by displacing the upper surface to the right by 0.015 mm. As with the compression deformation, all of the nodes are first moved to positions consistent with the applied strain and all of the interior nodes are subsequently released to relax to a static equilibrium configuration.

The shear stress computed from the virtual work relation, Eq. 16, is 0.01038036 MPa. Since there is no volume change associated with this deformation, the linearized energy relation corresponding to Eq. 18 is simply $e = 0.5\ A\ L_0 \sigma_{ev}\ \gamma_{ev}$ = 1.557054×10^{-4} N-mm, where $\gamma_{ev} = 0.015/2$ is the shear strain. The energy directly integrated by ParaDyn is 1.557843×10^{-4} N-mm, for an error of 0.05%. Here too, the proposed average stress calculation is shown to give a consistent result.

The normal-shear coupling of the irregular structure is also evident in the *x*-direction and *y*-direction stress for this simulation, shown in Table 2. It is also notable that the pressure, –1/3 the trace of the stress, is not zero, implying shear-pressure coupling. One might be tempted to cross-check the 2 analyses of the irregular structure by calculating the K_{2212} entry of the elastic stiffness from the second problem, which should be equal to the K_{1222} entry of the first problem if the elastic material is derivable from a strain energy relation. However, simple shear

involves a rotation of the stress tensor to satisfy material frame indifference, and that contribution to the *x*- and *y*-direction stresses is expected to be on the order of approximately 10^{-4} MPa, given the calculated RVE response. This unknown stress contribution is similar in magnitude to the stresses involved in the correlation, so such an analysis cannot be performed with any degree of certainty with the information currently available.

5.6 Deformation in the Plastic Range

The previous analyses demonstrated that the average stress calculate from virtual work relations, Eq. 16, provide an accurate RVE stress in the elastic range. However, the stress calculation does not depend on the material being elastic, as it is based only on the beam forces and geometry. The stress calculation will be equally valid if the beams are deformed into the plastic range. This is clearly evident for the 2-beam model where the RVE stress is computed directly from the forces and geometry. The irregular beam structure can also be evaluated in the plastic range, but the energy cannot be used for validation. Instead, validation must rely on the summation of nodal forces on the RVE surfaces. The force summation requires that the nodes on the lateral surfaces be free of shear tractions (Section 3), which is only appropriate for a limited range of deformation modes, as will be discussed Section 6.

A simulation similar to that of Section 5.4 was run with shear-free lateral surfaces. If the beam yield strength remains high, as it was for the analyses above, the response is elastic and the *y*-direction stress determined from the virtual stress relations, Eq. 16, is 0.03866 MPa. The force output in ParaDyn plots is available to only 3 digits. The sum of the *y*-direction forces on the upper surface divided by the 2-mm^2 surface area agrees with this stress to the first 3 digits, as expected. The analysis was repeated with a beam yield strength of 0.5 MPa, and the structure deformed plastically. Here the *y*-direction stress computed from the virtual work expressions is 0.004542 MPa. The stress computed from the summation of surface forces again agrees to the 3 available nonzero digits, confirming that the method does indeed calculate the correct stress in the plastic range.

The mass proportional damping applied to quell the dynamic modes alters the path dependence of the solution in the plastic range. While the path dependence of the solution is incorrect, the resulting configuration is still a valid static equilibrium configuration, and it is suitable for analysis stress averaging methods for the RVE.

6. Discussion

The decision to impose the boundary conditions on all of the exterior nodes of the RVE requires discussion. For uniaxial strain, allowing the nodes freedom to slide along the RVE surfaces does result in somewhat lower stress and elastic deformation energy, as noted in Section 5.6. These boundary conditions were investigated and the results are also consistent with stresses calculated by the virtual work expression, Eq. 16. However, it is not possible to apply shear free boundary conditions consistent with an arbitrary strain increment, as shear stresses cannot be supported, and a simple shear analysis would not be possible. Thus, an arbitrary strain can only be imposed consistently on the RVE by specifying boundary conditions on all of the degrees of freedom on all of the exterior nodes.

A consequence of these boundary conditions is that the stress cannot be calculated by summing forces over faces except, in special circumstances. Consider the configuration in Fig. 2. The *y*-direction forces on the lateral surfaces also contribute to the *y*-direction stress. The sums of the forces on the upper and lower surfaces are not necessarily the same, nor is the sum of forces over a face divided by the area necessarily equal to the average stress.

Another boundary condition choice that needs to be address concerns rotations and moments. No rotational constraints are imposed on the beam rotation degrees of freedom, and the resultant moments at static equilibrium are zero on all of the nodes, interior and exterior. Imposing rotation constraints on the exterior of the RVE results in moments on the exterior of the RVE. These contribute to an effective moment imposed on the RVE. In the derivation of the stress tensor for continuum mechanics, it is assumed that there is not net moment at a material point, and that assumption results in the stress tensor being symmetric. An RVE is treated as a material point from the perspective of the higher length scale model, so having a net moment on the RVE would be inconsistent with the underlying continuum mechanics assumptions.

Simulations on the beam configuration in Fig. 2 were run imposing constraints on the rotational degrees of freedom on the exterior nodes consistent with the applied deformation. For simple shear, these boundary conditions were no rotation on the upper and lower surface nodes, and nodal rotations equal to half of the shear angle on the lateral surfaces. The rotations of the corner nodes were the average of the 2 intersecting faces. When the volume-average stress was determined using virtual work relations, Eq. 16, the contribution from the first term of the $\bar{\sigma}_{xy}$ expression was different from the contribution from the second term in the first digit. Without

application of the rotation boundary conditions, the terms were the same to at least 7 nonzero digits. The imposed rotation constraints on the RVE inconsistent with the underlying continuum mechanics assumptions and the virtual work derivation. The classical derivation of the stress tensor is for a material point and assumes that summation of moments at the point is zero. That assumption leads to the stress tensor being symmetric. Moments resulting from imposition of rotation boundary conditions violate this underlying assumption, which is reflected in unequal contributions to the shear stress in Eq. 16. Since the higher length scale code in the HMS framework assumes a symmetric stress tensor, rotational constraints cannot be imposed for the current HMS framework.

Stepping back from the current application, there is nothing inherently wrong with a subscale microstructure model producing a nonsymmetric stress, traction gradients on the surfaces, and coupling between deformation modes. These features reflect aspects of microstructure in finite volumes that are not considered in the continuum mechanics derivations for behavior at a material point. The upper length scale analyses typically ignore the structure within RVEs because only the first moments of the response, the averages, can be used in the formulation. It should be possible to construct continuum-like frameworks with finite-sized base units rather than assuming reduction to a material point (couple-stress theories are still based on representations at a material point). These would have the potential to incorporate second moments of microstructure information into large-scale deformation analyses.

7. Conclusions

An efficient procedure has been presented to obtain the static equilibrium configuration of a network of elastic beams within an explicit dynamic finite element code. Expressions for computation of the average stress over the RVE have been presented based on the principal of virtual work, and these stresses have been shown to be consistent with both nodal force computations and stored energy. The stress averaging procedure is also valid for RVE deformations into the plastic range.

8. References

1. Knap J, Spear CE, Leiter KW, Becker R, and Powell DA. A computational framework for scale-bridging in multiscale simulations; 2014. Submitted for publication.

2. Bardenhagen S, Triantafyllidis N. Derivation of higher order gradient continuum theories in 2,3-d non-linear elasticity from periodic lattice models. J Mech Phys Solids. 1994;42:111–139.

3. Hughes TJR, Liu WK. Nonlinear finite element analysis of shells: part II. Two-dimensional shells. Comp Meths Appl Mechs. 1981;27:167–181.

4. Hill R. On constitutive macro-variables for heterogeneous solids at finite strain. Proc R Soc Lond A. 1972;326:131–147.

1 (PDF) DEFENSE TECHNICAL INFORMATION CTR DTIC OCA

2 (PDF) DIRECTOR US ARMY RESEARCH LAB RDRL CIO LL IMAL HRA MAIL & RECORDS MGMT

1 (PDF) GOVT PRINTG OFC A MALHOTRA

9 (PDF) DIR USARL RDRL CIH C J KNAP K LEITER C SPEAR RDRL WMP B C HOPPEL M KLEINBERGER A SOKOLOW RDRL WMP C R BECKER S BILYK T BJERKE

INTENTIONALLY LEFT BLANK.